IEEE Transactions on Geoscience and Remote Sensing Volume: 57 , Issue: 9 , Sept 2019

First Demonstration of Joint Wireless Communication and High-Resolution SAR Imaging Using Airborne MIMO Radar System

Jie Wang, Xing-Dong Liang, Long-Yong Chen, Li-Na Wang, and Kun Li

***Abstract*—Special attention has been devoted to joint wireless communication and radar sensing systems in recent years. However, since communication and radar have conflict requirements in terms of waveforms, transceiver developments, and signal processing algorithms, realization of this system concept is still a great challenge. In this paper, we introduce an airborne multi-input multi-output (MIMO) radar, along with the modified orthogonal frequency-division multiplexing (OFDM) and space–time coding (STC) waveform schemes, for the implementation of the joint wireless communication and synthetic aperture radar (SAR) imaging. The proposed system, which simultaneously transmits multidimensional waveforms with reconfigurable channels, can acquire adequate degrees of freedom. Thereby, it becomes a feasible method to perform both data transmission and high-resolution SAR imaging at the same time without intramodal interference. Theoretical analysis is validated by laboratory and flight experiments. Through our analysis, we aim to open up a new perspective of using MIMO radar to realize joint wireless communication and SAR imaging.**

***Index Terms*—Airborne multi-input multi-output (MIMO) radar, joint wireless communication and synthetic aperture radar (SAR) imaging, orthogonal frequency-division multiplexing (OFDM), space–time coding (STC).**

I. Introduction

RADAR systems have extensively contributed to a diverse range of scientific applications, including remote sensing missions [1]–[3]. Expanding the applications of radar systems, the fusion of radar sensing and wireless communication has become increasingly crucial for future missions [4]–[9]. The intelligent transportation applications, for example, require intelligent vehicles and traffic monitoring unmanned aerial vehicles (UAVs) to have the capability of autonomously sensing the driving environment and cooperatively exchanging information data, such as microwave traffic images, weather conditions, as well as entertainment content. Another example is wireless sensor networks [10] that demand individual nodes to detect targets and share its information with other nodes through wireless communication links. To this extent, the radar application can use the information distributed on the communication network to increase its detection probability and precision. Furthermore, future radar applications with wider swath and higher resolution would produce large amounts of raw data [11], [12]. The platforms, which can hardly burden the processing capacity, need to transmit the massive data to the base station for real-time processing. Even more important, if the concept of joint wireless communication and radar sensing is successfully implemented, the occupied spectrum would be used very efficiently, and the limited availability of spectral resources would partially overcome [13].

Accordingly, a number of papers focused on joint wireless communication and radar sensing have been published in the past decades. However, problems, such as the intramodal electromagnetic interference suppression and the functional reconfiguration, have not been settled. Implementation of this concept, which concerns waveform design and transceiver development, is still a great technological challenge. This is mainly because different underlying operation principles suggest different requirements. According to the fundamental limit studies of the shared spectrum access for radar and communications (SSPARCs) programs [14]–[16], the design requirements of radar and communications may conflict in both waveforms and radio frequency (RF) front-end architectures. Specifically, the waveform contradiction is more intense for the synthetic aperture radar (SAR) application that demands a much higher signal-to-clutter ratio (SCR) [17]. Conventional joint waveform schemes, which try to realize the communication and the SAR applications simultaneously with a single waveform, are not applicable. The interferences introduced from the wireless communication, which often appear as the high sidelobes in the range impulse response functions (IRFs), would definitely worsen the SCR. Moreover, the inconstant envelope characteristic of the communication

Manuscript received August 16, 2018; revised December 21, 2018 and February 25, 2019; accepted March 15, 2019. Date of publication May 20, 2019; date of current version August 27, 2019. This work was supported by the National Natural Science Foundation of China under Grant No. 61801228. *(Corresponding author: Xing-Dong Liang.)*

J. Wang and L.-N. Wang are with the School of Electronic and Information Engineering, Nanjing University of Information Science and Technology, Nanjing 210044, China.

X.-D. Liang and L.-Y. Chen are with the Science and Technology on Microwave Imaging Laboratory, Institute of Electronics, Chinese Academy of Sciences, Beijing 100190, China (e-mail: xdliang@mail.ie.ac.cn).

K. Li is with the Beijing Institute of Spacecraft System Engineering, Beijing 100094, China.

Color versions of one or more of the figures in this article are available online at http://ieeexplore.ieee.org.

Digital Object Identifier 10.1109/TGRS.2019.2907561

waveform also reduces the SAR power efficiency and the signal-to-noise ratio (SNR) [18].

It can be concluded from the earlier research that, due to the restricted degrees of freedom, the extremely high sidelobes, and the low power efficiency, the conventional multichannel systems with the joint waveforms cannot satisfy the design requirements of joint wireless communication and SAR imaging. However, multi-input multi-output (MIMO) radar systems with a phased array, which can acquire more degrees of freedom by simultaneously transmitting orthogonal waveforms in the same frequency band [19]–[23], show great potential. Since the multiple orthogonal waveforms, which are radiated by different antennas simultaneously, are designed to fulfill the conflict principles, respectively, the performance of the joint system can be optimized to its upmost, but the problem is that there are no such perfect orthogonal waveforms [24]–[26]. The matched filtering operations of the radar application would spread but not remove the energy of the communication signals in the time–frequency plane. This spread communication energy denotes the intramodal interference. It will be accumulated from numerous targets in the scene, and it degrades the SAR images significantly. However, it is fortunate to note that, from the viewpoint of the multidimensional modulation, multidimensional waveforms have emerged as potential solutions to suppress this kind of interference. Specially, the short-term shift-orthogonal (STSO) waveforms [27], [28] and the OFDM chirp waveforms [29]–[32] have already been successfully used to suppress the intrachannel interference in the MIMO-SAR systems.

In this paper, we explicitly propose the airborne MIMO radar, along with the multidimensional waveforms, to implement the application of joint wireless communication and SAR imaging. In particular, the joint waveform drawbacks and the multidimensional waveform advantages are analyzed, following which the orthogonal frequency-division multiplexing (OFDM) and the space–time coding (STC) waveform scheme are modified to suppress the intramodal interference. Performance of the modified OFDM waveforms has been verified by a laboratory experiment. As for the transceiver development, the multiple RF channels of an airborne MIMO radar system have been reconfigured. Based on that development, the STC scheme is validated via the flight experiments of the MIMO radar. The remainder of this paper is organized as follows. The waveform schemes are described in Section II, which is followed by the MIMO RF configuration in Section III. The experimental flight results are detailed in Section IV, and we present our conclusions in Section V.

II. Waveform Scheme

Since the concept of joint radar and communication was proposed, an important issue has arisen with regards to the waveforms. Some authors have suggested joint waveforms, including single-carrier and multicarrier schemes [8], [13]. These waveforms may be applicable for joint communication and traditional radar applications. However, they are not suitable for the fusion of SAR and wireless communication.

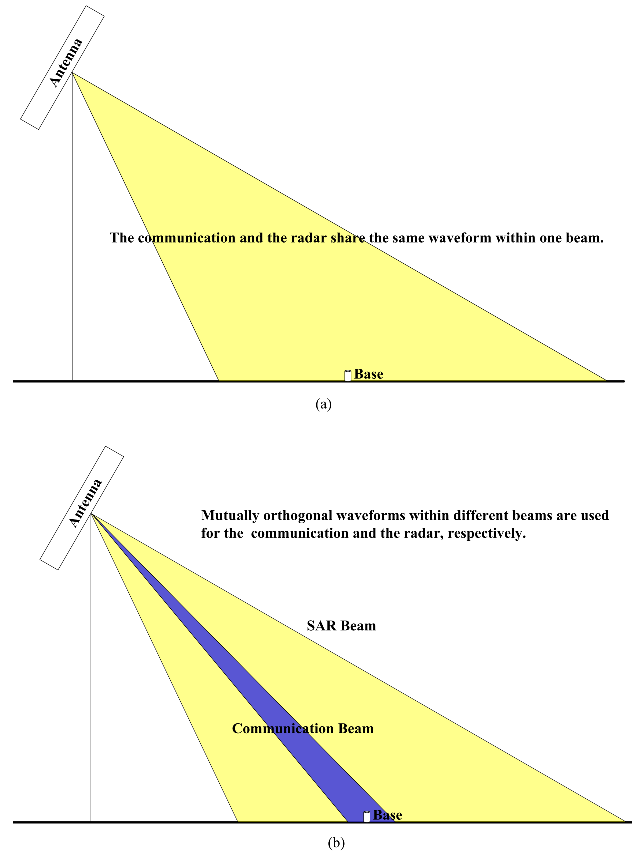

Fig. 1. Geometry of the joint communication and SAR system using (a) joint waveform in one beam and (b) orthogonal waveforms in multiple beams.

A. Joint Waveform Drawbacks

SAR waveform designers aim to create waveforms with optimum aperiodic autocorrelation properties that guarantee low sidelobes when applying correlation processing in the receiver. The constant signal envelopes in both time and frequency domains are also highly required for the maximum power efficiency and SNR. Presently, the most popular example fulfilling this requirement is the linear frequency modulated (LFM) signals. Hence, some authors have proposed the linear frequency modulation also for encoding communication data [7], [33]. In this approach, SAR and wireless communication can be performed simultaneously by a single waveform, and the performance of SAR imaging can be ensured due to the low sidelobes and the maximum power efficiency. However, from the communications perspective, the data rate is limited to the chirp rate [13], [33]. Moreover, since the communications share the same beam with the SAR [see Fig. 1(a)], and the latter prefers a wider coverage, the former security would be risked. It is not optimal for wireless communication.

In order to achieve better communications' performance, some authors have suggested improving the typical communication waveforms to meet the radar autocorrelation requirements. The spread spectrum signals with good periodic autocorrelation properties, for example, are the well-known candidate for joint radar and communications

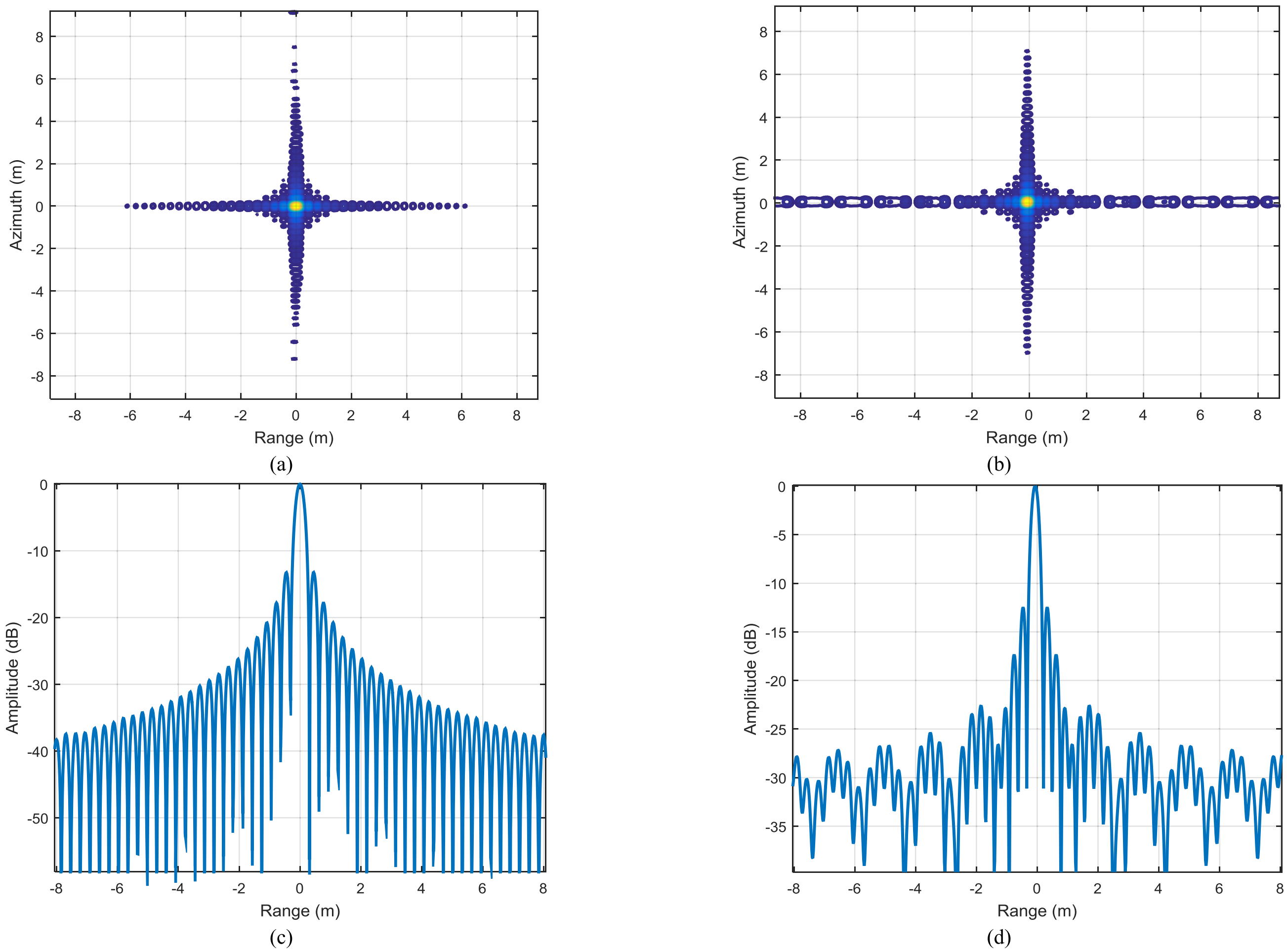

Fig. 2. Point-target simulation results of the classical LFM signals and the typical OFDM waveforms. (a) Simulation results of the LFM signals. (b) Simulation results of the typical OFDM waveforms. (c) Range profile of the simulation results shown in (a). (d) Range profile of the simulation results shown in (b).

applications [34]. Recently, multicarrier communication waveforms, which are regarded as the most promising ones for providing high performance in both radar and communications, have also received special attention [35]. For these waveforms, the sidelobes of the aperiodic autocorrelation function are high even if their periodic autocorrelation properties were optimal. However, with some processing techniques in the frequency domain, the sidelobes can be reduced to a certain extent. The impact of the reduced sidelobes may be negligible for the radar applications that focus on a sparse set of targets. However, when it comes to imaging every detail in the scene for SAR applications, this impact is fatal. It is mainly because the raised sidelobes from numerous targets would be accumulated. The accumulated sidelobes level, which may even exceed the energy of the focused low backscatter, significantly degrades SAR imagery. For instance, while the typical OFDM waveforms are well suited for wireless communication, their sidelobes are too high for SAR imaging [36]. It can be apparently found from the compression results of the classical LFM signals and the typical OFDM waveforms shown in Fig. 2. As a result, for the scene simulation of the typical OFDM waveforms shown in Fig. 3(b), the sidelobes from numerous targets have exceeded the energy of the focused weak backscatters and, significantly, deteriorated the SCR of the SAR images. In [37], more details about the joint waveforms' theoretical performance bounds with consideration to the sidelobes can be found.

Compared to the joint waveform schemes, the orthogonal waveforms may be better options for joint wireless communication and SAR imaging. The idea behind the orthogonal waveform scheme is to design multiple orthogonal waveforms for different modes to fulfill various principles. Since these waveforms share the same frequency band and are radiated by different antennas simultaneously, the performance of communication and SAR can be optimized to their upmost. Moreover, with the MIMO antenna configuration, the orthogonal waveforms can allow the joint system to perform the communication and the SAR application with different beams [see Fig. 1(b)]. In this case, the communication data will not be transmitted to each spot in the scene. Its security can be ensured.

However, theoretically, there is no such perfect orthogonal waveform [24]–[26]. According to the Ambiguity function defined by Woodward [38], if we matched the filter with the SAR signals, the energy of the communication waveforms is spread but not removed in the time–frequency plane.

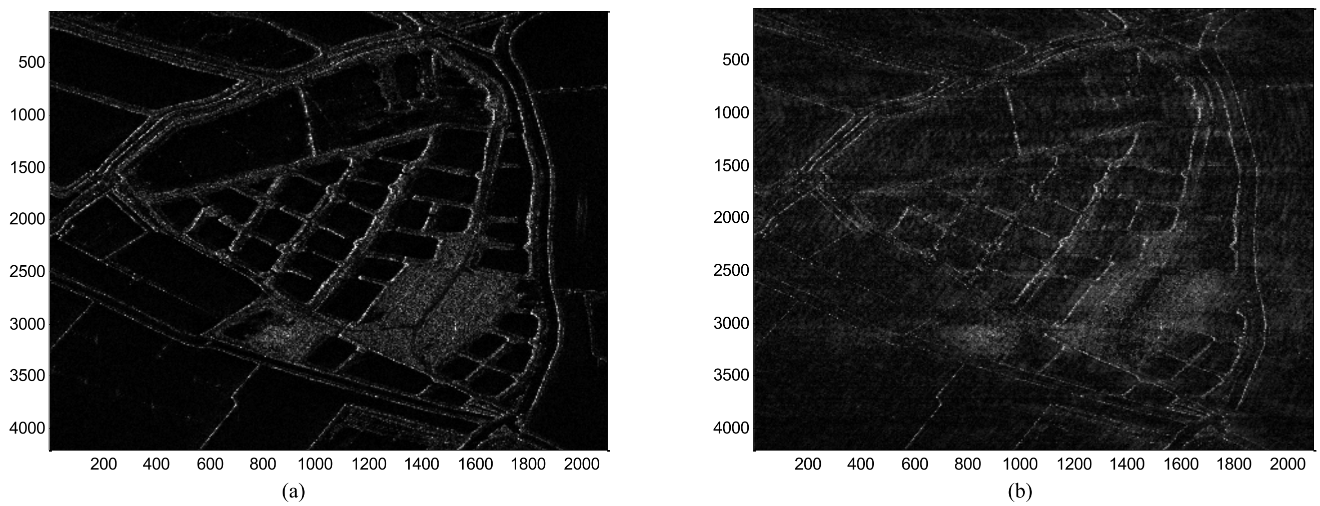

Fig. 3. Impact of the high sidelobes on the SAR imaging. (a) SAR image using chirp waveforms. (b) SAR image with typical OFDM waveforms.

The spread communication energy is the aforementioned ambiguous energy. It would be accumulated from numerous targets, and it degrades the SAR image. In fact, the impact of this ambiguous energy is just as the same as that of the high sidelobes waveforms.

In order to avoid the ambiguous energy, multidimensional waveform schemes, such as the STSO waveforms, the STC waveforms [39]–[43], and the OFDM chirp waveforms, have emerged as potential solutions. The essential difference between the multidimensional and the conventional orthogonal waveforms is that the multidimensional waveforms are modulated in multiple dimensions, including time, space, frequency, Doppler, polarization, and so on. Consequently, although the waveforms of SAR and communication share the same time–frequency coverage, they can still be perfectly separated by filtering in many other domains. To this extent, the electromagnetic interference between SAR and communication can be avoided, and the separated waveforms can be used for subsequent SAR and communication processing, respectively. In this paper, the OFDM and the STC waveform scheme are employed.

B. OFDM Waveform Scheme Used for Joint Wireless Communication and SAR Imaging

OFDM waveforms are initially used for the wireless communication. They can provide a number of advantages, such as the availability of processing gain, the perfect subcarriers orthogonality, and the reduction of power spectral density. The OFDM waveforms have also been proposed for the traditional radar applications. However, as mentioned earlier, the typical OFDM waveforms are not suitable for SAR imaging. To resolve this problem, the OFDM principle can be further combined with the LFM waveforms to exploit both the efficiency of data transmission and the useful characteristics of LFM signals, including the low sidelobes and the flat envelope. In particular, the LFM signals used for SAR imaging, and the signals carrying communication information are modulated into the odd and the even subcarriers of the OFDM waveform spectra, respectively. Since the subcarriers are orthogonal, the interference between the SAR and the communication can be avoided, and a better SAR imaging performance can be offered without degrading the symbol rate of the communication. Note that the basic idea of modulating the LFM signals into the OFDM subcarriers was initially proposed in [29] for MIMO-SAR imaging. In this paper, we will modify it for joint wireless communication and SAR imaging.

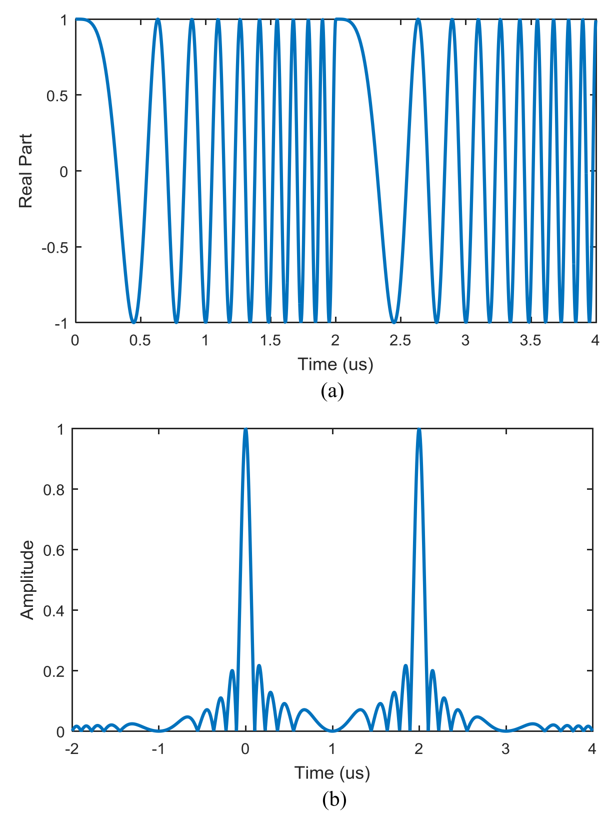

Fig. 4. OFDM waveforms for the SAR imaging. (a) Waveforms in the time domain. (b) Compression results.

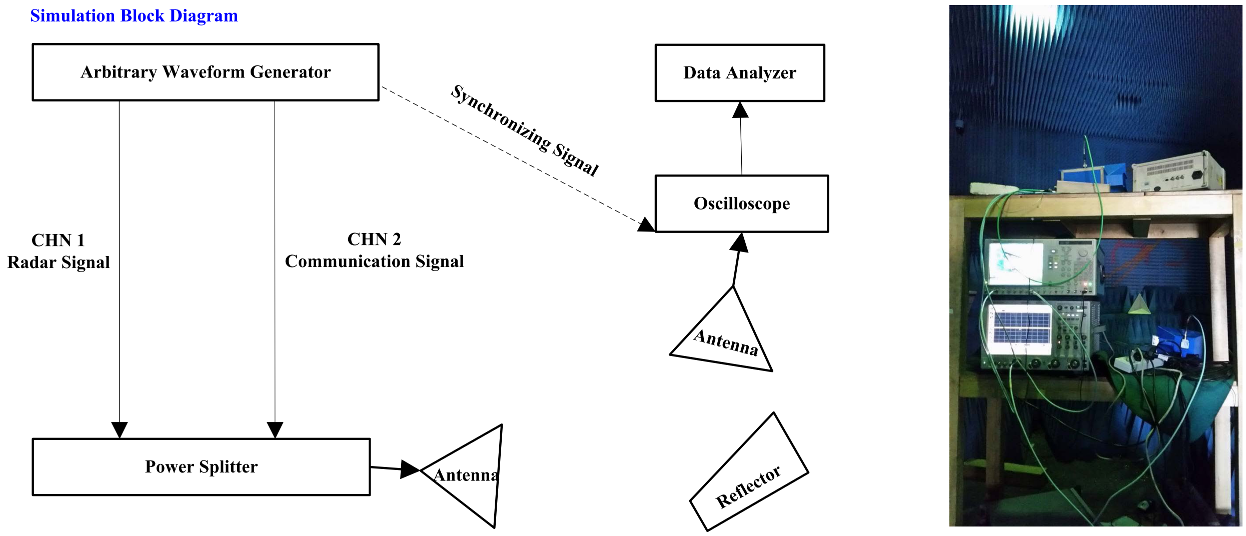

Fig. 5. Laboratory experiment with the proposed OFDM waveforms. The pulse duration and the bandwidth are 80 μs and 100 MHz, respectively.

Generally speaking, the generation of an OFDM multicarrier signal is realized by executing an inverse discrete Fourier transform (IDFT) on a defined data sequence. For simplicity, we assume that the duration of the OFDM waveform used for SAR imaging is $2T$, where T is the duration of the LFM signal to be modulated into the OFDM waveform. The communication waveform duration is $2T$ as well. Then, the data sequences are

$$\begin{aligned} \mathbf{X}_1(2p_1-1) &= \mathrm{DFT}\left[\exp\left(j\pi k_r\left(\frac{n-1}{F_s}\right)^2\right)\right], \quad \mathbf{X}_1(2p_1)=0 \\ \mathbf{X}_2(2p_1-1) &= 0, \quad \mathbf{X}_2(2p_1) \\ &= \mathrm{DFT}\left[s(n)\cdot\exp\left(-j\frac{2\pi}{2N}(n-1)\right)\right] \end{aligned} \tag{1}$$

where $\mathbf{X}_1$ and $\mathbf{X}_2$ are used to produce the SAR and the communication waveforms, respectively, $s(n)$ denotes the original communication signal, $p_1 = 1, 2, \ldots, N$, $n = 1, 2, \ldots, N$, $N = F_s \cdot T$, F_s denotes the sample rate, and k_r is the chirp rate.

By transforming (1) into the time domain, we can get the mutually orthogonal OFDM waveforms as follows:

$$\begin{aligned} x_1(t_r) &= \mathrm{rect}\left(\frac{t_r}{T}\right)\cdot\exp\left(j\pi k_r\cdot t_r^2\right) \\ &\quad + \mathrm{rect}\left(\frac{t_r-T}{T}\right)\cdot\exp\left(j\pi k_r\cdot(t_r-T)^2\right) \\ x_2(t_r) &= s(t_r) - s(t_r-T) \end{aligned} \tag{2}$$

where t_r denotes the fast time.

It can be seen from (2) that each of the OFDM waveforms consists of two successive identical subpulses. This repetition property has little impacts on the wireless communication that focuses on the direct waves. However, for the SAR imaging, it would introduce two peaks with T distance into the compressed echo of each point target [see Fig. 4(b)]. The maximum unambiguous swath, as a result, is restricted to $cT/2$, where c denotes the speed of light. Otherwise, there would be range ambiguities. That is to say, each point target would appear twice in the swath, and the first peaks of latter point targets will be aliased with the second peaks of the former ones. As a consequence, for the geometry shown in Fig. 1(b), the base station, on the one hand, can directly extract the even subcarriers from the superposed signals transmitted by the joint system to perform the demodulation procedure. On the other hand, the joint system, which tries to avoid the intramodal interference and the swath ambiguities, should first use the digital beam forming (DBF) technique in the elevation to divide the whole scene into multiple shorter subsets with T durations and then extract the odd and the even subcarriers, respectively, from the divided results to separate the radar echoes and the communication data transmitted from the communication base station.

Based on the developed OFDM waveform scheme, a laboratory experiment has been conducted to validate the performance. For simplicity, the DBF technique is not employed, and the swath is assumed to be narrower than $cT/2$. The simulation block diagram is shown in Fig. 5. It consists of an arbitrary waveform generator (AWG), a power splitter, an oscilloscope, a reflector, and two antennas. For the signals flowing in the simulation, the OFDM waveforms are generated by the AWG, superposed in the power splitter, and subsequently radiated by the antenna. The received signals captured by the receiving antenna are sampled by the oscilloscope. The simulation results are shown in Fig. 6.

It can be seen from the simulation results that the modified OFDM waveform scheme can offer a better range compression performance without degrading the communication data rate. Consequently, we can conclude from the theoretical analysis and the simulation that the OFDM scheme can be used for joint wireless communication and SAR effectively. However, as mentioned earlier, it should be combined with the DBF technique in the elevation direction for wider swath imaging. To this end, it is applicable for the airborne systems that

IEEE Transactions on Geoscience and Remote Sensing Volume: 57 , Issue: 9 , Sept 2019

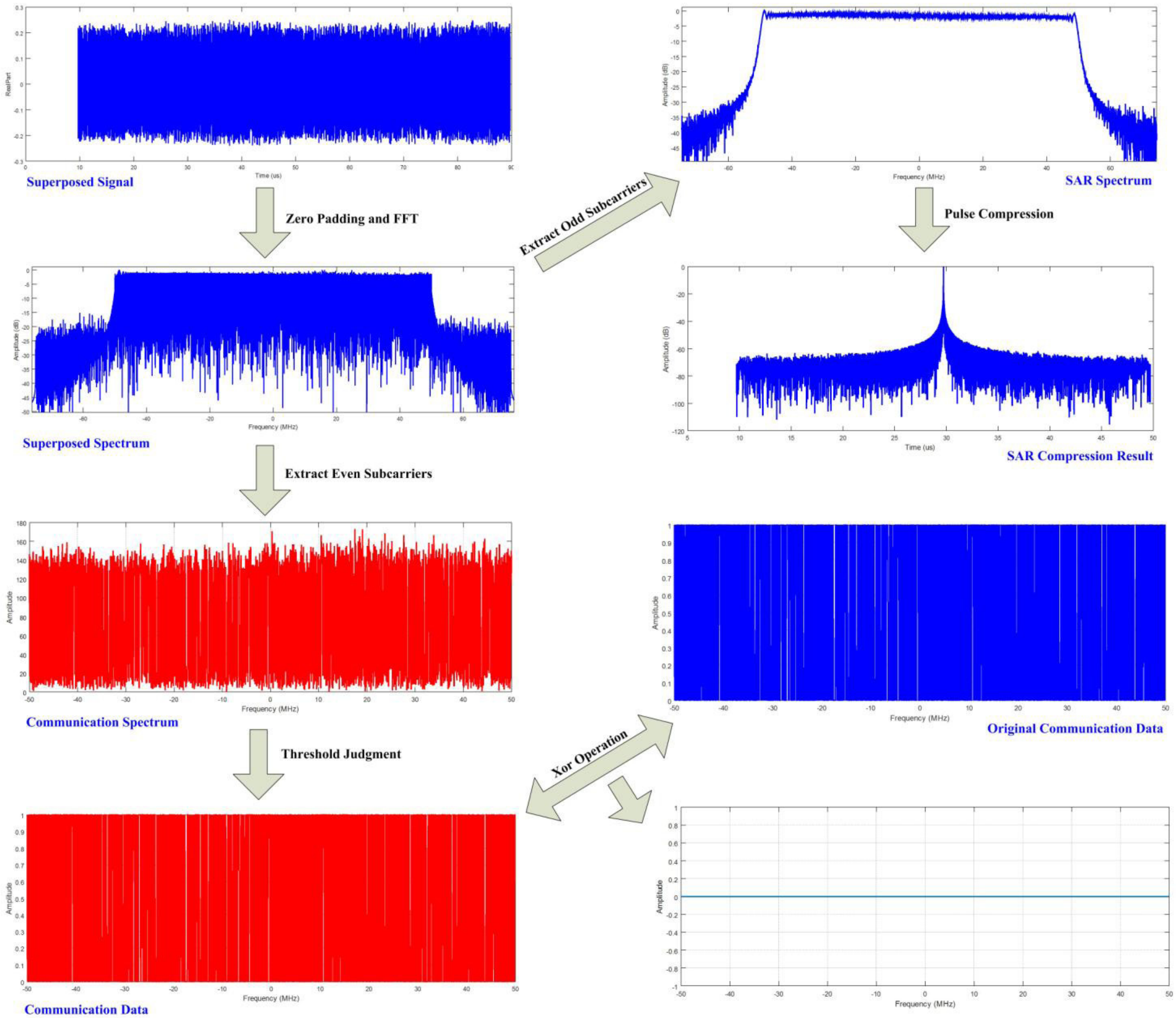

Fig. 6. Laboratory experimental results. The waveforms can simultaneously acquire 250-Mbit/s data rate and 1.5-m resolution in the simulation. Meanwhile, the sidelobes of the compression result and the envelope in the frequency domain remain consistent with those of a conventional LFM signal. Note that the XOR operation between the demodulated and the original communication data is employed because the XOR result can be used to compute the bit error rate (BER).

placing the antennas on the plane side. However, for the space-limited UAVs or the airborne systems mounting the antennas at the plane bottom, it would be infeasible. In order to resolve this problem, we will introduce another multidimensional waveform scheme, namely, the STC scheme, in Section II-C.

C. STC Waveform Scheme Used for Joint SAR Imaging and Wireless Communication in Space-Limited Platforms

Similar to the OFDM waveforms, the STC scheme has also received special attention in both the wireless communication and the radar fields. In particular, it has already been proposed for MIMO-SAR interferometry in [39] and owned a good performance in the case that the channel responses are constant during the consecutive transmissions. However, for the time-variant channel responses, which are mainly introduced by the flight motions or the other

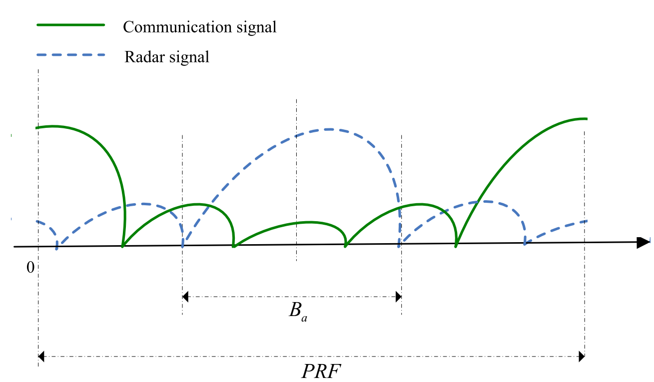

Fig. 7. STC configuration for joint wireless communication and SAR imaging.

factors, there would be residual ambiguous energy and “ghost targets.” In order to remove this restriction, we can modify

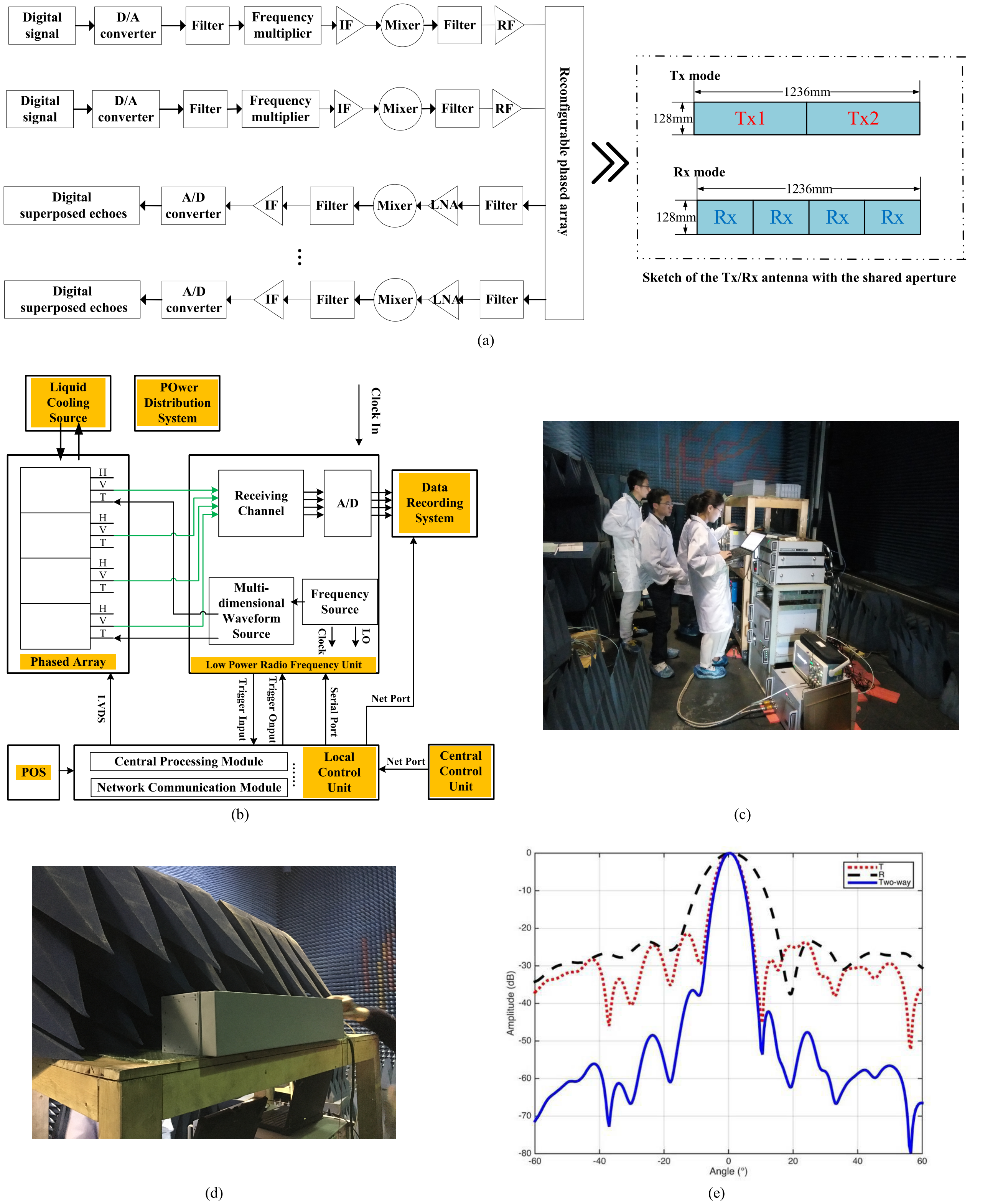

Fig. 8. MIMO RF configuration for joint wireless communication and SAR. (a) Signal flow diagram of the MIMO radar system. (b) MIMO radar system architecture. (b) MIMO radar system under test. (d) Photograph of the phased array. (e) Tested antenna patterns of the phased array.

the original Alamouti coding and decoding procedures and further improve them for the application of the joint wireless communication and SAR imaging systems in the space-limited flight platforms.

The signal model of the conventional STC scheme is based on the following 2×2 Alamouti coding matrix:

$$S = \begin{bmatrix} s_1 & s_2^* \\ s_2 & -s_1^* \end{bmatrix} \tag{3}$$

where $(\cdot)^*$ denotes the complex conjugate operator and s_1 and s_2 denote the basic signals.

We can specialize the basic signals as $s_1 = s_2^*$. Then, (3) can be rewritten as follows:

$$S = \begin{bmatrix} s_1 & s_2^* \\ s_2 & -s_1^* \end{bmatrix} = \begin{bmatrix} s_1 & s_1 \\ s_2 & -s_2 \end{bmatrix}. \tag{4}$$

The entries in the above-mentioned coding matrix denote the signals transmitted by the antennas. In particular, two different signals, namely, s_1 and s_2, are transmitted simultaneously from two distinct antennas during the first pulse repeat interval (PRI), following which s_1 and $-s_2$ are radiated by the same antennas.

For the side-looking geometry, the signals in the first row of (4) transmitted by one antenna can be rewritten as follows:

$$s_1'(t_r, t_a) = \omega(t_a) s_1(t_r) \tag{5}$$

where t_r denotes the fast time, t_a denotes the slow time, and $\omega(t_a)$ denotes the azimuth envelop.

The signal in the second row of (4) transmitted by another antenna can be rewritten as follows:

$$\begin{aligned} s_2'(t_r, t_a) &= \omega(t_a) \cdot s_2(t_r) \cdot \exp(jm\pi) \\ &= \omega(t_a) \cdot s_2(t_r) \cdot \exp(j2\pi f_{ac} t_a) \end{aligned} \tag{6}$$

where

$$f_{ac} = \frac{\mathrm{PRF}}{2}, \quad t_a = \frac{m}{\mathrm{PRF}} \tag{7}$$

pulse repetition frequency (PRF) denotes the pulse repeat frequency, and m is the sequence of sampled points in the slow time.

Then, for the nth antenna, the received data containing the superposed space–time coded signals are

$$r_n(t_r, t_a) = s_1'(t_r, t_a) \otimes h_{1,n}(t_r, t_a) + s_2'(t_r, t_a) \otimes h_{2,n}(t_r, t_a) \tag{8}$$

where $\otimes$ denotes a convolution and $h_{1,n}(t_r, t_a)$ denotes the channel response, including the spatially distributed targets backscattering characteristics, the atmosphere transmission property, the aircraft motion characteristics, and so on. It is related to the antenna transmitting the first row signals and the nth antenna. Similarly, $h_{2,n}(t_r, t_a)$ is related to the antenna transmitting the second row signals and the nth antenna.

Transform (8) into the Range-Doppler domain, we can get

$$\begin{aligned} R_n(t_r, f_a) = {} & s_1(t_r) \cdot W(f_a) \cdot H_{1,n}(t_r, f_a) \\ & + s_2(t_r) \cdot W(f_a - f_{ac}) \cdot H_{2,n}(t_r, f_a) \end{aligned} \tag{9}$$

where f_a denotes the azimuth frequency.

It can be seen from (9) that, for a given receiver, echoes related to different transmitters locate at different azimuth frequencies. Thus, instead of the Alamouti decoding, we can separate the multitransmitted signals by bandpass filtering in the Range-Doppler domain. To this end, the performance becomes independent of time-variant channel responses [41].

However, one cannot make an omelet without breaking eggs. This modified scheme has three drawbacks. First, the system PRF should be two times larger than the Doppler bandwidth to avoid the Doppler aliasing. Second, although the

(a)

(b)

Fig. 9. MIMO radar system loaded on the plane. (a) Phased array antennas outside the cabin. (b) MIMO radar system inside the cabin.

scheme can suppress the intramodal interference for the space-limited platforms, we cannot get the additional STC processing gain due to the unemployment of the Alamouti decoding. Last but not least, the sidelobes of the Doppler spectra, which are resulted from the antenna pattern in the azimuth direction, may introduce residual intramodal interference. The impact of the sidelobes will be further investigated in Section III.

Even more important, it should be noted that the modified STC scheme is based on the assumption that the basic signals s_1 and s_2 in the coding matrix are complex conjugate. Since the waveform design requirements of SAR and communication are conflict as mentioned earlier, this assumption cannot be fulfilled. For example, if the SAR signal is the complex conjugate of a typical communication signal, the imaging performance will be degraded by the high sidelobes and the low power efficiency. On the contrary, if the communication signal is a chirp form, the data rate will be reduced significantly. However, we can get rid of this assumption by starting the modulation directly from (5) and (6), which means that the SAR chirp signals are intrapulse modulated with an extra phase π and the OFDM signals used for communication remains the same within different PRIs [42]. To this end, the modified waveform scheme can also be derived from the azimuth phase coding technique proposed in [44]. Then, the communication signal locates at the baseband of the Doppler frequency, and the chirp signal used for SAR imaging locates at the high band (see Fig. 7). The interference between the SAR and the communication can be avoided. Moreover, with proper MIMO RF channel configuration (detailed in Section III), the data transmission efficiency of the

Fig. 10. Airborne geometry including the base station location.

OFDM-based communication signal and the low sidelobes, as well as the flat envelope, of the chirps can be exploited to simultaneously perform high-speed communication and high-resolution SAR imaging on a single MIMO system. This novel concept will be validated by the experimental flight results of an airborne MIMO radar system in Section IV.

III. MIMO RF Configuration

Apart from the electromagnetic interference suppression between the wireless communication and the SAR applications, the RF configuration is also essential for the implementation of the joint system. However, although the RF architectures in radar and wireless communication have become more and more similar in the current technological development, the joint RF channel (one RF channel simultaneously for communication and radar) could not be realized by the state-of-the-art technology. This is mainly because the communication and the SAR applications suggest conflict systematic requirements with regards to the transceiver developments, especially the amplification ones. For example, while the SAR applications prefer a saturation amplification to guarantee maximum power efficiency and SNR, the communications demand a linear amplification to avoid distortion. Since the linear and the saturation amplifications cannot be performed simultaneously by one channel, we are unable to transmit the SAR and the communication signals through the so-called joint channel. Otherwise, either the communication or the SAR performance would be degraded. In order to resolve this problem, the multiple reconfigurable transmitting channels of an airborne MIMO radar system will be introduced in this paper. It is especially true for the communication, where one of the channels is accommodated to produce a linear amplification by controlling the amplitude of the digital signal.

The MIMO radar system is shown in Fig. 8. This radar is a reconfigurable MIMO system, which mainly consists of the phased array antenna, the low-power RF unit, the data recording system, and the local control unit [see Fig. 8(b)]. In particular, there are two transmitting channels and four receiving ones in the low-power RF unit. The waveforms in the channels are generated at intermediate frequencies (IFs), upconverted to RFs, and subsequently radiated by the antenna. The received RF signals captured by the receiving antennas are downconverted to an IF after being amplified. The IF signals are then sampled by the A/D converter. The signal flow diagram of the system is shown in Fig. 8(a). As for the phased array antenna, it is divided into two subapertures when it transmits signals and reconfigured as four subapertures when it receives the echoes. The photograph of the array is shown in Fig. 8(d). The beam widths of the phased array in the horizontal direction are $4.2°$ and $8.4°$, respectively. Its total length is about 1.2 m. Based on the phased array, we have tested the antenna pattern in the horizontal direction to evaluate the influence of the Doppler spectra sidelobes on the STC scheme. The results of the tested patterns are shown in Fig. 8(e). It can be seen from results that the normalized amplitude of the sidelobes in the two-way antenna pattern is lower than -40 dB. Thus, if the STC scheme is employed, we can conclude that the residual intramodal interference introduced by the sidelobes of the Doppler spectra would be negligible.

By employing the above-mentioned MIMO RF configurations, both of the OFDM and the STC schemes can be used to realize the concept of joint wireless communication and SAR imaging. However, the OFDM waveform scheme, which would not double the system PRF, is the first choice for the wider swath purpose. However, as mentioned earlier, it should be combined with the DBF technique in the elevation direction

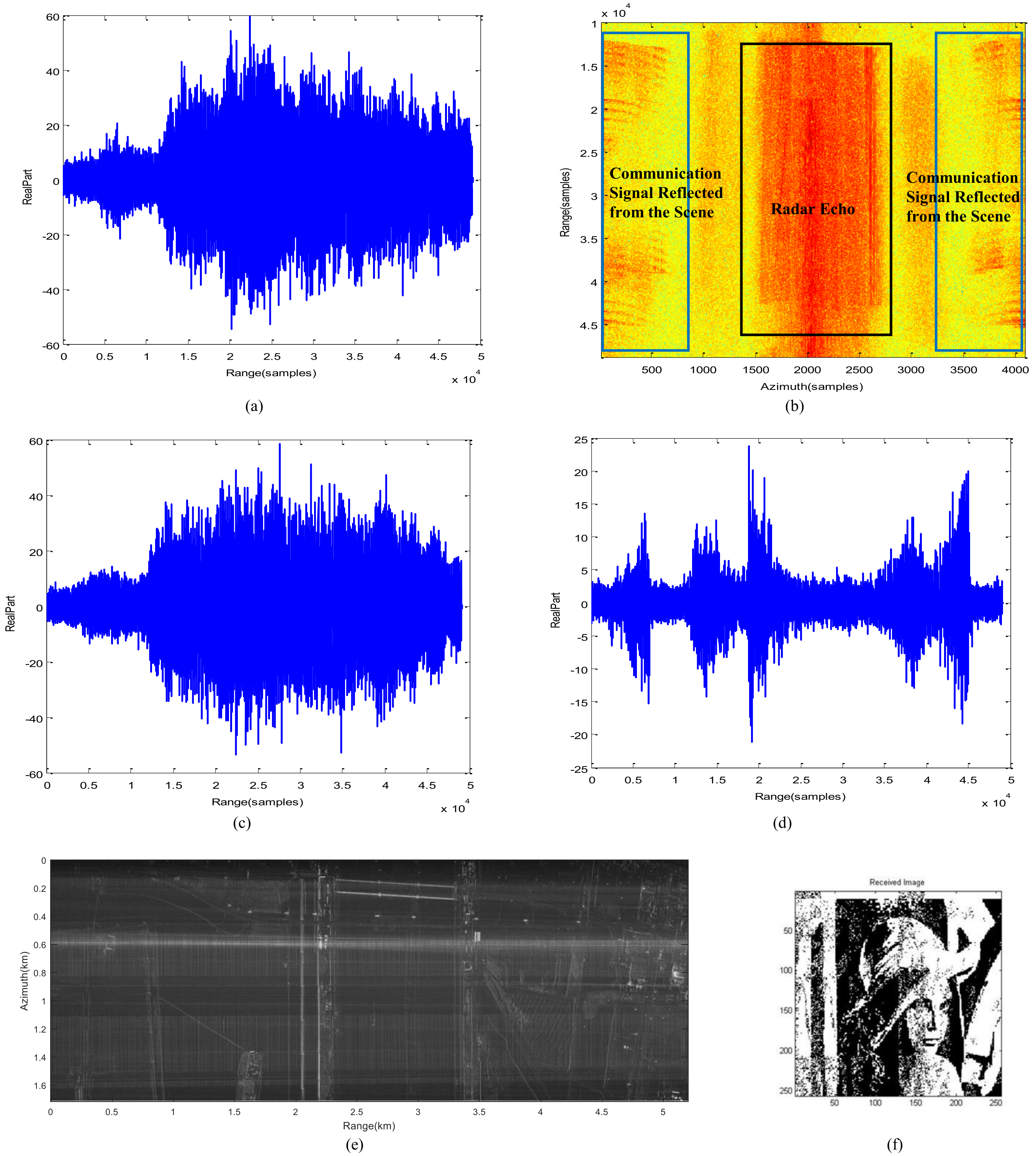

Fig. 11. Experimental flight results. (a) Superposed echoes in the time domain at a certain azimuth position. (b) Superposed echoes in the Range-Doppler domain. (c) Separated radar signal at the same azimuth position of (a) and (b). (d) Separated communication signals reflected from the scene. (e) Reconstructed SAR image affected by the communication mode. (g) Reconstructed SAR image with the STC configuration. (f) and (h) Sent and received images in the communication mode, respectively. (i) Azimuth averaged energy of (e) and (g). (j) and (k) SAR IRFs in the range and the azimuth direction, respectively.

to avoid the range ambiguities. To this end, the phased array should be installed vertically at the aircraft bottom. As an alternative, we can also draw on the successful experience of the PARMIR system to mount the phased array antennas vertically into the aircraft door [45]. As for the modified STC scheme, the phased array installation is relatively simple. It can be installed at the aircraft bottom along the azimuth direction.

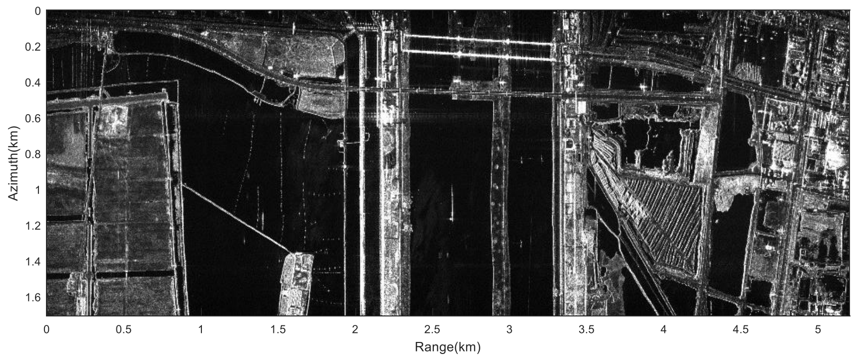

(g)

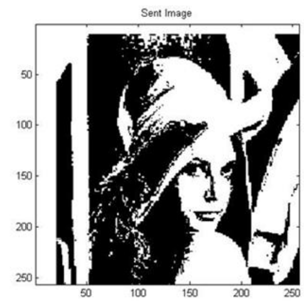

(h)

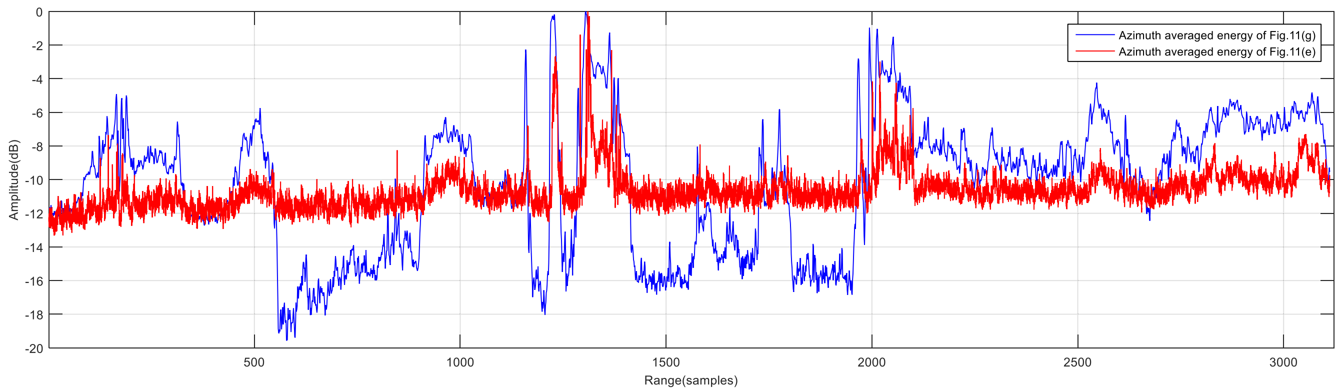

(i)

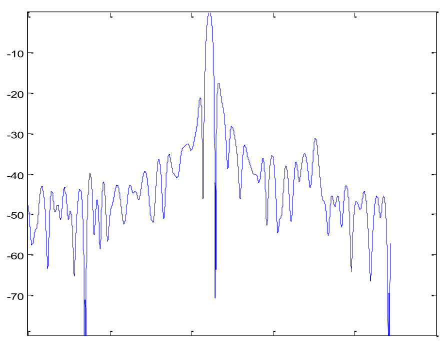

(j)

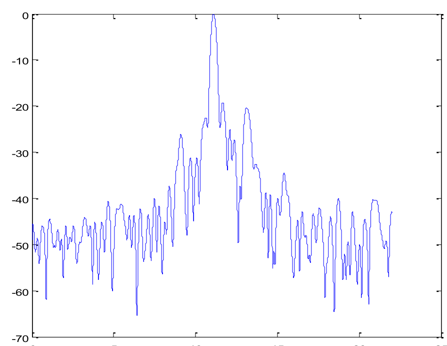

(k)

Fig. 11. *(Continued.)* Experimental flight results. (a) Superposed echoes in the time domain at a certain azimuth position. (b) Superposed echoes in the Range-Doppler domain. (c) Separated radar signal at the same azimuth position of (a) and (b). (d) Separated communication signals reflected from the scene. (e) Reconstructed SAR image affected by the communication mode. (g) Reconstructed SAR image with the STC configuration. (f) and (h) Sent and received images in the communication mode, respectively. (i) Azimuth averaged energy of (e) and (g). (j) and (k) SAR IRFs in the range and the azimuth direction, respectively.

IV. Experimental Flight Results

To validate the MIMO-implemented concept of joint wireless communication and SAR imaging, flight experiments were conducted. The plane that is used to perform the flight experiment is shown in Fig. 9. Since the flight height is 8 km and the plane needs to balance its inner pressure, we cannot mount the arrays into the parachute door of the aircraft. In addition, the distance between the plane belly and the ground is limited. The phased array antennas, whose total length is about 1.2 m, cannot be placed at the plane bottom along the elevation direction. As a consequence, the OFDM scheme, which should be combined with the DBF technique in the elevation direction to avoid the range ambiguities, cannot be realized in the flight experiment. Then, the STC scheme, along with the phased array antennas mounted at the plane bottom along the azimuth direction, is used for the validation. In this case, the chirp signal used for the SAR imaging locates at the high band in the Doppler frequency domain. The typical OFDM communication signal locates at the baseband of the Doppler frequency. Since the chirp and the OFDM signals modulated into the STC scheme are the optimal waveforms for the SAR and the wireless communication and they can be separated by bandpass filtering in the Range-Doppler domain, the performance of the joint system can be optimized to its upmost.

TABLE I
PARAMETERS OF AIRBORNE MIMO RADAR SYSTEM

Total duration (R/C)	75us/35us
Signal bandwidth (R/C)	560MHz
Carrier frequency	5.4GHz
Sampling frequency	1.5GHz
Platform Height	8km
Doppler bandwidth	480Hz
Sub-antenna Length	0.3m
Pulse Repeat Frequency	2000Hz

Parameters used in the flight experiments are shown in Table I, where R and C denote the radar and the communication, respectively. While the durations are different, their bandwidths are the same. In addition, the radar maximum power is 1800 W. This experiment was performed at Tianjin, China. The airborne geometry, including the base station location, is shown in Fig. 10. The flight results are shown in Fig. 11.

It can be seen from Fig. 11(a) that, since the proposed system simultaneously transmits multimodal waveforms with multiple channels, the echoes are superposed in the time domain. And if the multidimensional waveform designed in this paper is not employed, the communication signals, which are transmitted from the joint system to the base station and then reflected from the scene, would introduce severe electromagnetic interference into the SAR receiving channel. This interference significantly degrades SAR images [see Fig. 11(e)]. However, by employing the STC configuration, the reflected communication signals and the SAR echoes can be separated because the superposed data are disjoint in the Range-Doppler domain [see Fig. 11(b)]. As a result, the intrachannel electromagnetic interference has been suppressed. And the performance of the SAR imaging and the wireless communication can be ensured in Fig. 11(g) and (h). The performance improvements of the multidimensional waveform over the conventional one are more obvious in the figures of the SAR azimuth averaged energy [see Fig. 11(i)]. Moreover, for the parameters in Table I, we can acquire about 0.3-m resolution in both directions.

Note that Fig. 11(f) and (h) are the radar transmitted and the base station received communication images, respectively. These images are the firsthand results. Their quality will be further improved by employing the cyclic redundancy coding (CRC) and the channel estimation procedure in the future work. This experiment aims to validate the feasibility of the concept.

It can be concluded from the experimental flight results that the electromagnetic interference between the communication and the SAR applications can be suppressed by the STC scheme even though the oppressive jammer mode is employed. Consequently, we can realize joint wireless communication and high-resolution SAR imaging in the same frequency band through a single MIMO radar system.

V. CONCLUSION

Joint systems with wireless communication and radar sensing capability have aroused research interest over the past decades. Various modulation schemes and RF architectures have been proposed and studied to integrate or fuse these two functions in a single transceiver. Some authors even suggest one RF channel with a single waveform providing communication and radar applications simultaneously. These concepts may be applicable for radar applications that focus on a sparse set of targets. However, for SAR systems that aim to image every detail in the scene, the high sidelobes and the low power efficiency would degrade the performance significantly.

In this paper, from the viewpoint of the multitransceiver and multidimensional waveforms, we propose MIMO radar systems for the implementation of joint wireless communication and SAR imaging. Specifically, different waveforms are designed for different modes to fulfill various principles. The essence is that these waveforms are mutually orthogonal in multiple domains. As a result, when they are simultaneously transmitted by different RF channels that fulfill the conflict amplification requirements, the multimodal waveforms can be separated without electromagnetic intrachannel interference, and the performance of the communication and the SAR can be optimized to their upmost. Following that concept, the OFDM and the STC waveform schemes are modified. Both of the modified waveform schemes are applicable to the joint systems. However, the developed OFDM waveform scheme needs adequate space to place the array in the elevation direction for the DBF operation. The modified STC, which is suitable for space-limited platforms, would double the PRF and degrade the processing gain introduced by the Alamouti decoding. Then, the STC scheme is employed in the airborne experiment due to the limited belly space of the plane. The OFDM waveform scheme, as a result, is just validated by a laboratory experiment. Both of the experimental results have shown that the MIMO radar system can not only produce high-resolution SAR images but also provide wireless communication functionalities at the same time with little innerinterference.

VI. ACKNOWLEDGMENT

The authors would like to thank the anonymous reviewers for their valuable comments and suggestions.

REFERENCES

[1] F. Ulaby and D. Long, *Microwave Radar and Radiometric Remote Sensing*. Ann Arbor, MI, USA: Univ. Michigan Press, 2014.

[2] S. Huber, F. Q. de Almeida, M. Villano, M. Younis, G. Krieger, and A. Moreira, "Tandem-L: A technical perspective on future spaceborne SAR sensors for earth observation," *IEEE Trans. Geosci. Remote Sens.*, vol. 56, no. 8, pp. 4792–4807, Aug. 2018.

[3] M. Villano, G. Krieger, M. Jäger, and A. Moreira, "Staggered SAR: Performance analysis and experiments with real data," *IEEE Trans. Geosci. Remote Sens.*, vol. 55, no. 11, pp. 6617–6638, Nov. 2017.

[4] G. Krieger *et al.*, "MirrorSAR: A fractionated space radar for bistatic, multistatic and high-resolution wide-swath SAR imaging," in *Proc. IGARSS*, Fort Worth, TX, USA, Jul. 2017, pp. 149–152.

[5] A. R. Chiriyath, B. Paul, and D. W. Bliss, "Radar-communications convergence: Coexistence, cooperation, and co-design," *IEEE Trans. Cogn. Commun. Netw.*, vol. 3, no. 1, pp. 1–12, Mar. 2017.

[6] J. R. Guerci, R. M. Guerci, A. Lackpour, and D. Moskowitz, "Joint design and operation of shared spectrum access for radar and communications," in *Proc. IEEE Radar Conf. (RadarCon)*, Philadelphia, PA, USA, May 2016, pp. 1–6.

[7] G. N. Saddik, R. S. Singh, and E. R. Brown, "Ultra-wideband multi-functional communications/radar system," *IEEE Trans. Microw. Theory Techn.*, vol. 55, no. 7, pp. 1431–1437, Jul. 2007.
[8] L. Han and K. Wu, "Joint wireless communication and radar sensing systems - state of the art and future prospects," *IET Microw. Antennas Propag.*, vol. 7, no. 11, pp. 876–885, Aug. 2013.
[9] C. W. Rossler, "Adaptive radar with application to joint communication and synthetic aperture radar," Ph.D. dissertation, Dept. Elect. Comput. Eng., Ohio State Univ., Columbus, OH, USA, 2013.
[10] M. Vossiek, L. Wiebking, P. Gulden, J. Wieghardt, C. Hoffmann, and P. Heide, "Wireless local positioning," *IEEE Microw. Mag.*, vol. 4, no. 4, pp. 77–86, Dec. 2003.
[11] M. Younis, C. Fischer, and W. Wiesbeck, "Digital beamforming in SAR systems," *IEEE Trans. Geosci. Remote Sens.*, vol. 41, no. 7, pp. 1735–1739, Jul. 2003.
[12] A. Currie and M. A. Brown, "Wide-swath SAR," *IEE Proc. F Radar Signal Process.*, vol. 139, no. 2, pp. 122–135, Apr. 1992.
[13] C. Sturm and W. Wiesbeck, "Waveform design and signal processing aspects for fusion of wireless communications and radar sensing," *Proc. IEEE*, vol. 99, no. 7, pp. 1236–1259, Jul. 2011.
[14] G. M. Jacyna, B. Fell, and D. McLemore, "A high-level overview of fundamental limits studies for the DARPA SSPARC program," in *Proc. IEEE Radar Conf. (RadarConf)*, Philadelphia, PA, USA, May 2016, pp. 1–6.
[15] A. R. Chiriyath, B. Paul, and D. W. Bliss, "Joint radar-communications information bounds with clutter: The phase noise menace," in *Proc. IEEE Radar Conf. (RadarConf)*, Philadelphia, PA, USA, May 2016, pp. 1–6.
[16] C. D. Richmond, P. Basu, R. E. Learned, J. Vian, A. Worthen, and M. Lockard, "Performance bounds on cooperative radar and communication systems operation," in *Proc. IEEE Radar Conf. (RadarConf)*, Philadelphia, PA, USA, May 2016, pp. 1–6.
[17] J. C. Curlander and R. N. McDonough, *Synthetic Aperture Radar Systems and Signal Processing*. New York, NY, USA: Wiley, 1991.
[18] N. Levanon and E. Mozeson, *Radar Signals*. Chichester, U.K.: Wiley, 2004.
[19] E. Fishler, A. Haimovich, R. Blum, D. Chizhik, L. Cimini, and R. Valenzuela, "MIMO radar: An idea whose time has come," in *Proc. IEEE Radar Conf.*, Apr. 2004, pp. 71–78.
[20] J. Ender, "MIMO-SAR," in *Proc. Int. Radar Symp.*, Cologne, Germany, 2007, pp. 667–674.
[21] M. Younis, G. Krieger, and A. Moreira, "MIMO SAR techniques and trades," in *Proc. EuRAD*, Nuremberg, Germany, Oct. 2013, pp. 141–144.
[22] W.-Q. Wang, "Large-area remote sensing in high-altitude high-speed platform using MIMO SAR," *IEEE J. Sel. Topics Appl. Earth Observ. Remote Sens.*, vol. 6, no. 5, pp. 2146–2158, Oct. 2013.
[23] J. H. G. Ender and J. Klare, "System architectures and algorithms for radar imaging by MIMO-SAR," in *Proc. IEEE Radar Conf.*, Pasadena, CA, USA, May 2009, pp. 1–6.
[24] G. Krieger *et al.*, "MIMO-SAR and the orthogonality confusion," in *Proc. IGARSS*, Munich, Germany, pp. 1533–1536, Jul. 2012.
[25] G. Krieger, "MIMO-SAR: Opportunities and pitfalls," *IEEE Trans. Geosci. Remote Sens.*, vol. 52, no. 5, pp. 2628–2645, May 2014.
[26] B. Zou, Z. Dong, and D. Liang, "Design and performance analysis of orthogonal coding signal in MIMO-SAR," *Sci. China Inf. Sci.*, vol. 54, no. 8, pp. 1723–1737, Jun. 2011.
[27] G. Krieger, N. Gebert, and A. Moreira, "Multidimensional waveform encoding: A new digital beamforming technique for synthetic aperture radar remote sensing," *IEEE Trans. Geosci. Remote Sens.*, vol. 46, no. 1, pp. 31–46, Jan. 2008.
[28] T. Rommel, A. Patyuchenko, P. Laskowski, M. Younis, and G. Krieger, "An orthogonal waveform scheme for imaging MIMO-radar applications," in *Proc. IRS*, Dresden, Germany, Jun. 2013, pp. 917–922.
[29] J.-H. Kim, M. Younis, A. Moreira, and W. Wiesbeck, "A novel OFDM chirp waveform scheme for use of multiple transmitters in SAR," *IEEE Geosci. Remote Sens. Lett.*, vol. 10, no. 3, pp. 568–572, May 2013.
[30] J. Wang, X. Liang, C. Ding, L. Chen, L. Zhou, and Y. Dong, "An improved OFDM chirp waveform used for MIMO SAR system," *Sci. China Inf. Sci.*, vol. 57, no. 6, pp. 1–9, Jun. 2014.
[31] J. Wang, L.-Y. Chen, X.-D. Liang, C.-B. Ding, and K. Li, "Implementation of the OFDM chirp waveform on MIMO SAR systems," *IEEE Trans. Geosci. Remote Sens.*, vol. 53, no. 9, pp. 5218–5228, Sep. 2015.
[32] J. H. Kim, M. Younis, A. Moreira, and W. Wiesbeck, "Spaceborne MIMO synthetic aperture radar for multimodal operation," *IEEE Trans. Geosci. Remote Sens.*, vol. 53, no. 5, pp. 2453–2466, May 2015.
[33] S. D. Blunt, P. Yatham, and J. Stiles, "Intrapulse radar-embedded communications," *IEEE Trans. Aerosp. Electron. Syst.*, vol. 46, no. 3, pp. 1185–1200, Jul. 2010.
[34] K. Mizui, M. Uchida, and M. Nakagawa, "Vehicle-to-vehicle communication and ranging system using spread spectrum technique," in *Proc. IEEE 43rd Veh. Technol. Conf.*, pp. 335–338, May 1993.
[35] B. J. Donnet and I. D. Longstaff, "Combining MIMO radar with OFDM communications," in *Proc. Eur. Radar Conf.*, Sep. 2006, pp. 37–40.
[36] D. Garmatyuk and M. Brenneman, "Adaptive multicarrier OFDM SAR signal processing," *IEEE Trans. Geosci. Remote Sens.*, vol. 49, no. 10, pp. 3780–3790, Oct. 2011.
[37] B. Paul, A. R. Chiriyath, and D. W. Bliss, "Joint communications and radar performance bounds under continuous waveform optimization: The waveform awakens," in *Proc. IEEE Radar Conf. (RadarConf)*, Philadelphia, PA, USA, May 2016, pp. 1–6.
[38] P. Woodward, "Radar ambiguity analysis," RRE, New York, NY, USA, Tech. Rep. 731, Feb. 1967.
[39] J.-H. Kim, A. Ossowska, and W. Wiesbeck, "Investigation of MIMO SAR for interferometry," in *Proc. Eur. Radar Conf.*, Munich, Germany, Oct. 2007, pp. 51–54.
[40] F. He, Z. Dong, and D. Liang, "A novel space–time coding Alamouti waveform scheme for MIMO-SAR implementation," *IEEE Geosci. Remote Sens. Lett.*, vol. 12, no. 2, pp. 229–233, Feb. 2014.
[41] J. Wang *et al.*, "A novel space–time coding scheme used for MIMO-SAR systems," *IEEE Geosci. Remote Sens. Lett.*, vol. 12, no. 7, pp. 1556–1560, Jul. 2015.
[42] C.-Z. Meng *et al.*, "MIMO-SAR waveform separation based on inter-pulse phase modulation and range-doppler decouple filtering," *Electron. Lett.*, vol. 49, no. 6, pp. 420–422, Mar. 2013.
[43] W.-Q. Wang, "Space–time coding MIMO-OFDM SAR for high-resolution imaging," *IEEE Trans Geosci. Remote Sens.*, vol. 49, no. 8, pp. 3094–3104, Aug. 2011.
[44] J. Dall and A. Kusk, "Azimuth phase coding for range ambiguity suppression in SAR," in *Proc. IGARSS*, Anchorage, AK, USA, Sep. 2014, pp. 1734–1737.
[45] H. Wilden, O. Saalmann, B. Poppelreuter, O. Peters, and A. Brenner, "A radar frontend with time steered array antenna for PAMIR," in *Proc. EuMA*, Munich, Germany, pp. 202–205, Oct. 2007.

Jie Wang was born in Jiangsu, China, in 1986. He received the B.Sc. degree in information engineering from the Nanjing University of Information Science and Technology, Nanjing, China, in 2010, the M.Sc. degree in signal and information processing from the University of Chinese Academy of Sciences, Beijing, China, in 2013, and the Ph.D. degree in signal and information processing from the Science and Technology on Microwave Imaging Laboratory, Institute of Electronics, Chinese Academy of Sciences, University of Chinese Academy of Sciences, in 2015.

Since 2017, he has been with the School of Electronic and Information Engineering, Nanjing University of Information Science and Technology. His research interests include radar waveform designing and processing, joint communication and radar system engineering, and novel radar imaging techniques, such as multi-input multi-output and orthogonal frequency-division multiplexing, and cognitive synthetic aperture radar systems.

Xing-Dong Liang received the Ph.D. degree from the Beijing Institute of Technology, Beijing, China, in 2001.

Since 2002, he has been with the Institute of Electronics, Chinese Academy of Sciences, University of Chinese Academy of Sciences, Beijing, where he is currently a Professor and the Director of the Science and Technology on Microwave Imaging Laboratory. During this period, he has product responsibility for many important Chinese national programs, including high-resolution synthetic aperture radar (SAR) systems, polarimetric and interferometric SAR systems, and preresearch for advanced SAR systems. His research interests include real-time radar signal processing, coherent polarimetric and interferometric SAR systems, and novel radar imaging techniques.

Dr. Liang has been rewarded by the Chinese government for his great contributions to the remote sensing area for several times.

Long-Yong Chen received the B.Sc. degree in electrical engineering from the University of Science and Technology of China, Hefei, Anhui, China, in 2003, and the M. Sc. and Ph.D. degrees in signal and information processing from the University of Chinese Academy of Sciences, Beijing, China, in 2006 and 2009, respectively.

Since 2009, he has been with the Science and Technology on Microwave Imaging Laboratory, Institute of Electronics, Chinese Academy of Sciences, University of Chinese Academy of Sciences, where he is currently an Assistant Professor and the Assistant Director. During this period, he has product responsibility for millimeter-wave radars, receivers, polarimetric and interferometric synthetic aperture radar (SAR) systems, and multi-input multi-output SAR systems. His research interests include radar signal processing, coherent polarimetric and interferometric SAR system designing, and novel radar imaging techniques.

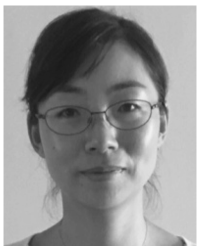

Li-Na Wang was born in Shanxi, China, in 1979. She received the B.S. degree in computer application from the Nanjing Institute of Meteorology, Nanjing, Jiangsu, China, in 2001, the M.S. degree in system analysis and integration from the Nanjing University of Information Science and Technology, Nanjing, in 2004, and the Ph.D. degree in computer application technology from the Nanjing University of Aeronautics and Astronautics, Nanjing, in 2016.

Her research interests include data mining, artificial intelligence, and cognitive communication processing.

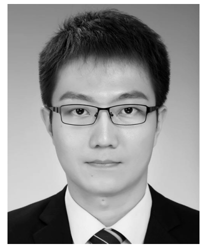

Kun Li received the Ph.D. degree in signal and information processing from the Science and Technology on Microwave Imaging Laboratory, Institute of Electronics, Chinese Academy of Sciences, University of Chinese Academy of Sciences, Beijing, China, in 2017.

Since 2017, he has been with the Beijing Institute of Spacecraft System Engineering, Beijing. His research interests include spaceborne radar system engineering and signal processing, high-resolution wide swath synthetic aperture radar (SAR) imaging, and distributed microsatellites SAR systems.